

OTTO LAPORTE MEMORIAL LECTURE

SHOCK TUBES IN FLOW LASER RESEARCH; MODELING AND APPLICATION

R. I. Soloukhin

Heat and Mass Transfer Institute, Minsk, USSR

A survey is given on the present state of development and some recent advances in the use of shock tubes to simulate typical processes and operation heated molecular gas mixtures. We show that specific laser energies of 25 Joules/gram can be extracted and gains as high as 3.5 m^{-1} were obtained in the mixed flow GDL systems with selective high-temperature excitation of the pumping component of the lasing mixture (e.g. nitrogen). We also present and discuss experimental data on measurements of spatial gain distributions behind a shock or rarefaction wave generated in the laser cavity flow, and of the resonance absorption coefficients of CO_2 at high temperatures.

Pioneering contributions of Professor Otto Laporte in the field of high temperature gas dynamics and spectroscopy of shock tube flows were continuously followed by systematic studies of gas flows involving well-pronounced radiant energy transport phenomena. In recent years this area has been substantially complemented by investigations concerned with the production and use of non-equilibrium molecular gas flows yielding vibrational-state population inversions and lasing. Some of the evident advantages associated with the use of shock tubes to generate non-equilibrium gas flows as follows: (i) simple operating conditions allow the attainment of high enthalpies in the working substance at mass flow rates of 1-10 kg/s and higher; (ii) achievement of a wide range of well determined temperatures and pressures in the plenum chamber, and (iii) obviating the requirement for high-power heating and cooling systems that are needed for steady flow supersonic wind tunnels or combustors. In shock tube flow lasers, molecular relaxation and reaction kinetics, convective and radiative energy transfer, as well as optical characteristics of the gaseous medium are closely related to the fluid mechanical behavior of the working substance. In addition it is possible to combine the shock tube with reliable optical systems to attain coherent radiation. Though usually, the quasi-steady state durations in the shock tube nozzle are only of the order of several milliseconds, these systems do simulate completely the operational regimes of cw gasdynamic lasers pumped by purely thermal means.

Operation of the gasdynamic lasers is substantially affected by gasdynamic disturbances generated in the supersonic flow of the vibrationally frozen working gas passing the laser cavity. Moreover resonance light absorption of gas samples having no population inversion seems also to affect the laser power extraction. Here again, the shock tube is one of the useful devices that provides wide temperature and pressure ranges in systematic studies of optical characteristics of high temperature radiative gas samples. This lecture reviews the present state of development and some advances in the use of shock tubes to simulate the typical operating regimes and processes in cw gasdynamic lasers, and to study the optical properties of shock-heated molecular gas mixtures. The paper is by no means meant to be an exhaustive survey, the choice of the material being limited mainly by the personal interest of the author and his co-workers as well as by some publications of Soviet contributors in this field. Recent comprehensive reviews on similar topics are now available and can be found in [1-6].

GASDYNAMIC CONSIDERATIONS

The shock tube gasdynamic laser is simply a conventional shock tube that provides a chosen molecular gas mixture at the desired reflected shock temperature and pressure. The reflected shock region serves as driver for a combination of a transition nozzle section, a laser cavity, and an evacuated dump tank. The shock tube channel is separated from the remaining sections by a diaphragm to minimize the starting time of the supersonic nozzle flow. Typically, a uniform flow is maintained through the nozzle for several milliseconds, being terminated by wave interactions in the shock tunnel. An essential difference of this design from traditional high speed supersonic shock tube wind tunnels is the flow channel geometry: the laser cavity channel cross-section is to be rectangular and highly extended in the direction of the cross-flow laser cavity. This requirement is somewhat inconsistent with the ordinary shock tube constructions, and therefore, various ways of their modification were used as illustrated in Fig. 1: (i) the rectangular shock tube channel followed by a slit-throat two-dimensional nozzle [7, 8], (ii) a slit [9–11] or a slit-throat supersonic nozzle mounted at the end of a large diameter circular shock tube [12–14], and (iii) circular-to-rectangular flow transition sections including the double-expansion principle [1, 15–17].

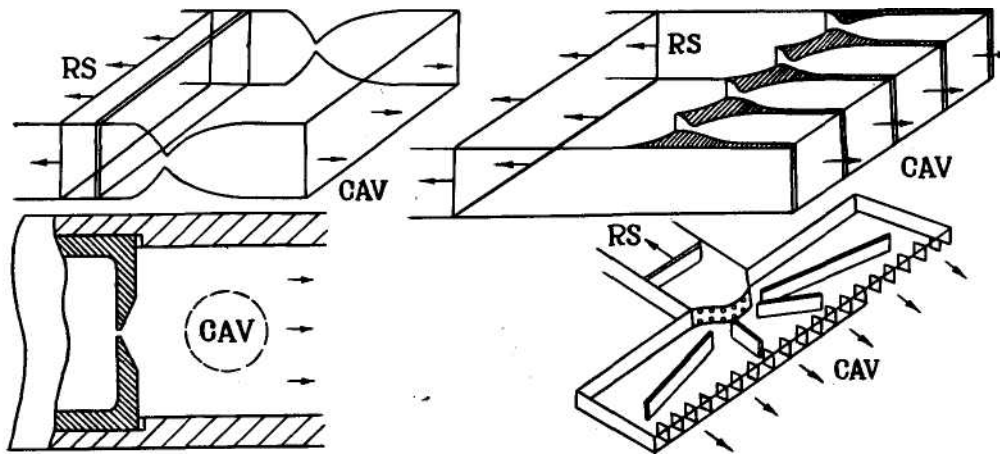


Fig. 1. Typical schematics of the GDL nozzle mounts in shock tubes:
(1) - [7], (2) - [20], (3) - [9–11], (4) - [16]

In the last case, a two-meter wide laser cavity combined with a four-inch diameter high pressure shock tube was operated with a nozzle assembly consisting of 100, $2 \cdot 10 \text{ cm}^2$ nozzles [16].

The starting process of a nozzle initiated by a shock wave is a complex non-stationary, two or three-dimensional gas dynamic phenomenon. A simplified quasi-steady flow approach based on the wave "tailoring" procedure (so called "Vector Polar" method [18]) was shown to be a good approximation in the wave interaction analyses allowing evaluation of basic gasdynamic parameters of this process.

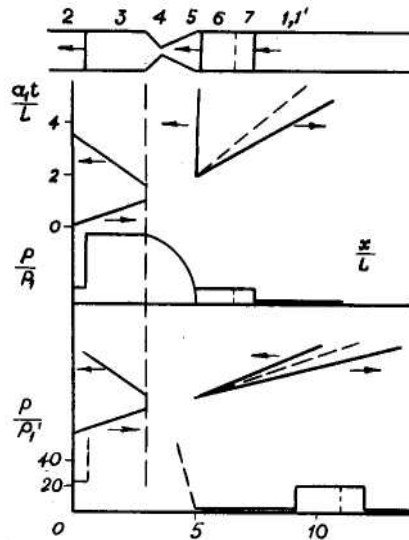


Fig. 2. Calculated wave and pressure diagrams illustrating typical GDL starting regimes. The nozzle and cavity sections are evacuated in the second regime [19]

The calculated wave and pressure diagrams illustrating two typical GDL starting regimes are shown in Fig. 2 [19]. In the first case, no diaphragm was placed ahead of the nozzle (area ratio 16:1:16), whereas in the second regime the nozzle area was evacuated to a pressure of $10^{-3} p_1$. A significant difference exists between the "secondary" shock speeds, u_s , in these two cases: $u_s' = 0.03a_1$ and $u_s'' = 2.56a_1$, respectively, where a_1 is the sound velocity of the driven gas. Thus, it is seen that an auxiliary diaphragm and a dump tank should always be used in GDL shock tube experiments to keep the starting time short (usually, about 10^{-4} sec). The corresponding experimental data are well described by this "Vector Polar" method. It was also proven [7, 8, 15, 16] that in a conventional shock tube with a driven section of 3–5 m length, the uniform quasi-steady flow is maintained through the nozzle for about 1.5–2.5 msec.

The performance of a GDL is highly influenced by the rate of expansion and freezing of the gases through a minimum length contoured supersonic nozzle. A variety of GDL nozzles, nozzle arrays, and nozzle-perforated plates were investigated to determine the optimum operational regimes [12–17, 20–25]. If one simply assumes that the nozzle flow is one-dimensional while the medium behaves essentially as a perfect gas with constant specific heat ratio, γ , then the translational temperature decreases with the nozzle length, l , at a rate which is determined by the semi-apex angle, α , as follows from [19],

$$\frac{T}{T_0} = \frac{2}{\gamma + 1} \left[\frac{\gamma - 1}{\gamma + 1} \left(1 - \frac{T}{T_0} \right)^{-1} \left(\frac{h_*}{h_* + 2l \tan \alpha} \right)^2 \right]^{\frac{\gamma - 1}{2}},$$

where T_0 is the gas temperature in the plenum chamber, h_* is the nozzle throat width. On this basis, the criterion for effective gasdynamic freezing can be expressed in terms of a "critical" freezing length, l_c , the distance behind the nozzle throat where the relative temperature decrease $\Delta T/T$ is of an order of unity. Thus, for $\gamma = 1.5$, one gets $l_c = (1.1 \div 2.4) h_*$ for $\alpha = 30^\circ$ and $\alpha = 15^\circ$,

respectively. In this evaluation, the effects of subsonic freezing in the inlet part of the nozzle are not included. At gas temperatures of about 2000 K, characteristic relaxation times of vibrational states in a "coupled" molecular system, e.g. $\text{CO}_2(001)+9\text{N}_2(v=1)$ are given by the relation [20], $p\tau_v$ (atm.sec) $\approx 10^{-5}$. Hence, for an expansion through a nozzle with $\alpha = 30^\circ$ the gas flow velocity $u \approx 1.5$ km/sec; assuming a pressure of $p = 0.5 p_0 = 10$ atm, we find that effective freezing should take place at a maximum distance, $l_c \sim u\tau_v \sim 1.5$ mm. According to the above relation, the maximum allowable throat width is fixed at $h_* \approx 1$ mm. This critical value determines all other geometrical parameters of the gasdynamic laser. Certainly, a more detailed analysis of the freezing in a gasdynamic laser nozzle will have to include both equations for the flow dynamics and vibrational relaxation kinetics [3, 4, 13, 26–36]. However, as a result, almost the same value for $h \approx 1$ mm will be obtained. Note that the freezing conditions are less strict if only pure nitrogen is expanded. Due to its low relaxation rate, N_2 could be frozen at the high temperature of the plenum [8], whereas it is usually assumed in equilibrium throughout the subsonic flow region.

On the basis of simplified conservation equations for a quasi-one-dimensional non-equilibrium nozzle flow one can estimate the maximum energy stored in the upper vibrational states of N_2 and CO_2 and the maximum available gain of the lasing gas under various plenum and freezing conditions. These estimates provide values for the important parameters that define the basic features of the GDL energetics and efficiency under various thermal and gasdynamic conditions.

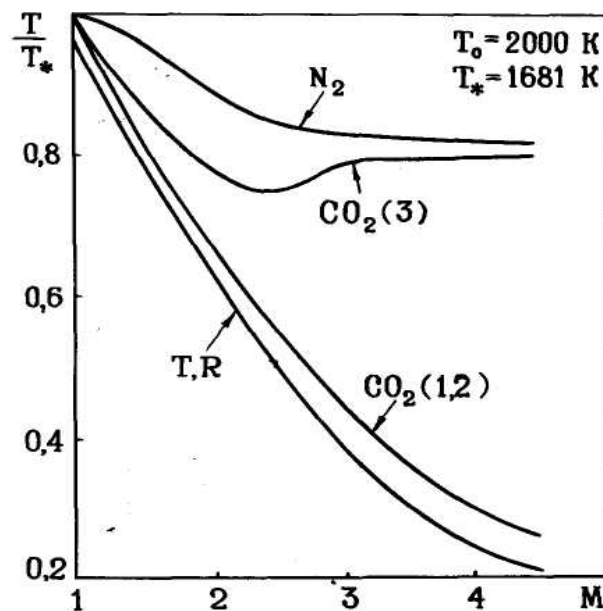


Fig. 3. Temperatures of various vibrational modes in a $\text{CO}_2\text{-N}_2$ molecular system as a function of the nozzle flow Mach number [32]

For instance, Figure 3 shows the gasdynamic laser freezing efficiencies at different flow Mach numbers. In this figure we plot the temperatures of various vibrational levels of the CO₂-N₂ system as well as translational temperature of the expanded and frozen gas as a function of the nozzle flow Mach number [32]. In view of the necessity to make the mass flow rate and gas density as high as possible in order to obtain high laser power output levels, a flow Mach number between M = 3.5 and 5 is seen to be the most preferable for efficient freezing. This means that supersonic area ratios of $h/h_* = 15 \div 30$ are typical for the GDL nozzles, i.e. the exit nozzle height is limited to a value of several centimeters. The calculated maximum available power per unit mass is shown in Fig.4 as a function of plenum gas temperature for different Mach numbers [35].

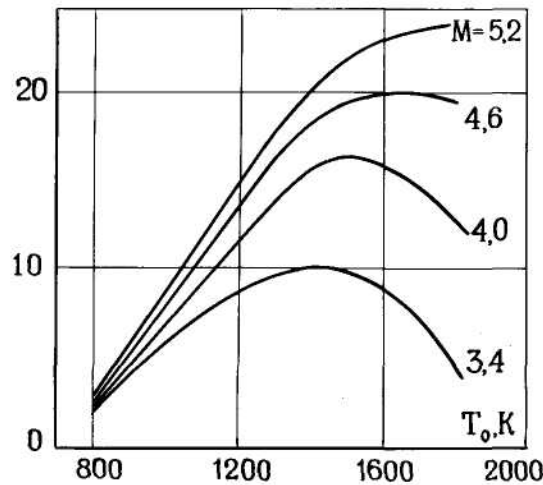


Fig. 4. Calculated maximum available power in a premixed GDL, as a function of plenum gas temperature, at different Mach numbers [35]; $p_0 h_*/\tan \theta = 2.26 \text{ atm.cm}$, gas mixture: $0.03 \text{ CO}_2 + 0.012 \text{ H}_2\text{O} + 0.958 \text{ N}_2$

These data also allow one to make the proper choice for the gasdynamic and thermal conditions that provide the optimum operational regime for a gasdynamic laser.

SHOCK TUBE LASERS: TYPICAL PERFORMANCE AND ADVANCES

Using the gasdynamic approach [37, 38] a population inversion in a thermally pumped molecular gas system was successfully obtained in a shock tube by several investigators [1, 9, 12, 16, 19]. Subsequently, gain measurements and laser power extraction simulation were also carried out by the use of the shock tube technique. The most impressive results were obtained with the use of a high pressure shock tube operating in a double expansion flow regime at mass flows of 50 kg/sec and specific extracted output energies of 8J/g. These results were reported at previous Shock Tube Symposium [16]. Not only shock tubes but also fast combustion and detonation processes were used to provide thermal pumping for appropriate gas mixtures. Some of these combustion driven pulsed GDL designs are shown schematically in Fig. 5 [39–43]. The largest of these systems [43] employs mixtures of acetylene, propane, and carbon monoxide with air. The gas mixture is exploded at initial pressure of 3 atm in a combustion chamber to provide a plenum

gas at pressures of 10 atm and temperatures of 1400–1700 K. Output power levels of 8.5 kW, specific extracted energies of 9.7J/g, and gain coefficients of 0.8 cm⁻¹ were attained. The steady flow duration was about 20 msec in this design.

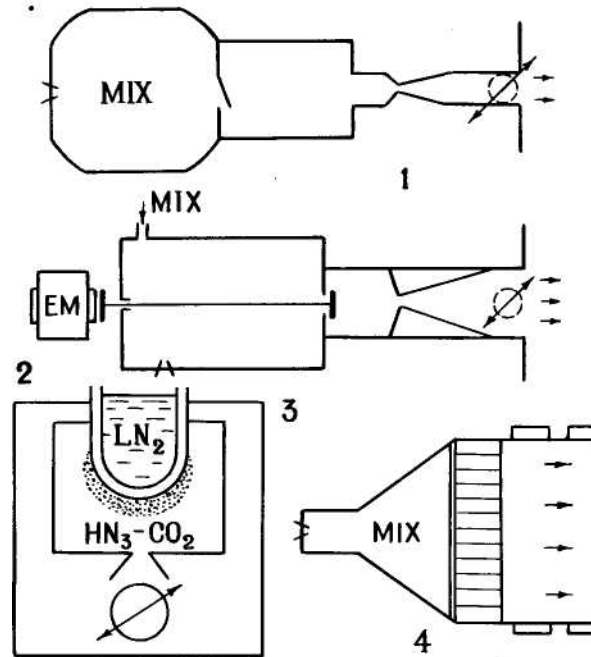


Fig. 5. Combustion and detonation driven GDL designs:
 (1) – [40], (2) – [41], (3) – [39], (4) – [43]

In order to compare basic parameters, output power characteristics, and efficiencies of the numerous GDL systems developed up to date in various laboratories we provide a systematic list in Table 1. From Table 1 it can be seen that the highest values of the basic parameters attained in conventional GDL systems are limited to gain coefficients of $\alpha \approx 1 \text{ m}^{-1}$, specific extracted energy of $\varepsilon \approx 8 \text{ J/g}$, and overall efficiencies of less than 0.5 per cent. These maximum values correlate well with their theoretical predictions [34]. They also illustrate the limited capacity of thermally excited molecular gas lasers operated at relatively low reservoir temperatures. We will not consider here the technological problems and difficulties that arise when we try to obtain a complete extraction of the vibrational energy that is available in the carrier gas. In the following we shall describe certain efforts that were made to avoid the basic limitations of the conventional GDL devices. These limitations are related to the relatively low thermal vibrational energy stored in the CO₂-N₂ system at temperatures below 2300 K. Above this temperature the dissociation of the CO₂ molecules and collisional deactivation effects become intolerable, in addition the relative populations of the working CO₂ vibrational levels decrease at higher temperatures. Thus, a concept of separately pumping pure nitrogen and injecting CO₂ downstream of the nozzle throat was conceived. This modified GDL nozzle design allowed the use of nitrogen plenum temperatures as high as 4000 K or higher [7, 8, 44–48].

Table 1

Mixture Comp CO ₂ :N ₂ :He /or H ₂ O/	T ₀	P ₀ atm	h A/A	Cavity- area cm ²	α_{\max} m ⁻¹	P _{max} kW	P/G J/g	η %	Refs.
7.5 :91 .3 :1 .2	14 00	17	0.8 14	2 0×8 0	0.8	60	4	0.4	20 1970
10:40:50	1200- 3400	13-18	1.27 20	2.5×14	-	0.25	2		12 1970
12:34 :54	800- 2200	2 -16	1 36.1	3.6×30	0.6	2	9		34 1972
22:73:5	1200- 1550	10	0.23 30	1.1×10	1	0.05	2		77 1971
10:30:60	2000- 4000	100	0.35 44.4	1.6×14	-	2.29	3.6		21 1972
6.8:68.2 :25	2000	1000	1 20	10×200	-	4 00	8		16 1973
10:20:70	1460	8.4	1.3 15	0.7×9	1.1	.015	0.15		78 1976
CO ₂ :N ₂ :He	1400- 1700	5-10	0.4 25	5×50	0.8	8.5	10	0.6	43 1975
25 :50:25	650		0.8 4		0.5	5	1		74 1975
5 :15 :80	2100	85	12.7 10			2	2.2	0.17	52 1972
N ₂ CO ₂ +He mixing	2000- 4000	10	0.8	5×12	3	2	25	1 .6	47 1973
N ₂ CO ₂ +He mixing	2000- 4000	10	1	3×12	2-3.5	2	25	1 .6	45 1973
N ₂ CO ₂ +H ₂ O mixing	2000	66	d = 0.4	2×28	1.5		26		75 1976
N ₂ +Ar CO ₂ +He mixing	2000- 3000	3-6	1 M=3.5- 4.5	1 .2×3.5	3	.071	23		76 1977
F ₂ +H ₂ , D ₂ SF ₆ +He + O ₂ chem.mix.	2 000	1 .3	36 slits	1.27× 17.6		2	24 3	9.8	6 1973
F+H ₂ , D ₂ F ₂ +He chem.mix.	134 0	6.5	50 slits	1 .9× 22.9		15.5	344	14 .7	6 1973

The shock tube technique was used in simulations of flow phenomena in chemical and downstream mixing gasdynamic lasers. Some details of the downstream mixing GDL concept and operation have been reported at one of the previous Shock Tube Symposia [45] and elsewhere [8, 47, 48]. This approach is considered now to be an effective way to drastically improve the power and efficiency of a thermally pumped GDL. The use of separate thermal pumping provides high reservoir temperatures of the nitrogen, and, therefore, effective freezing.

Moreover, rather high densities of the lasing gas can be obtained due to low final translational temperatures of the expanded mixture. The maximum efficiency, i. e. ratio of the available laser energy to the pumping gas enthalpy, is calculated to be as high as 6% in this operational regime whereas this efficiency is limited to a value of less than 2% in an ordinary premixed GDL device. A fast operating valve is employed in shock tube mixing lasers to provide one of the reacting components, or the cold working gas (CO_2) to be injected into the nozzle throat simultaneously or before the arrival of the main flow at the nozzle of the shock tube channel. A fast solenoid valve is proved to be a suitable device [7]. Its operating time was about 10^{-4} sec. It was triggered by the main shock tube diaphragm rupture.

Various supersonic mixing regimes were tested to find optimum operational conditions for the mixed flow GDL. The results are shown schematically in Fig. 6 where the measured spatial gas distributions are presented for three different injection systems.

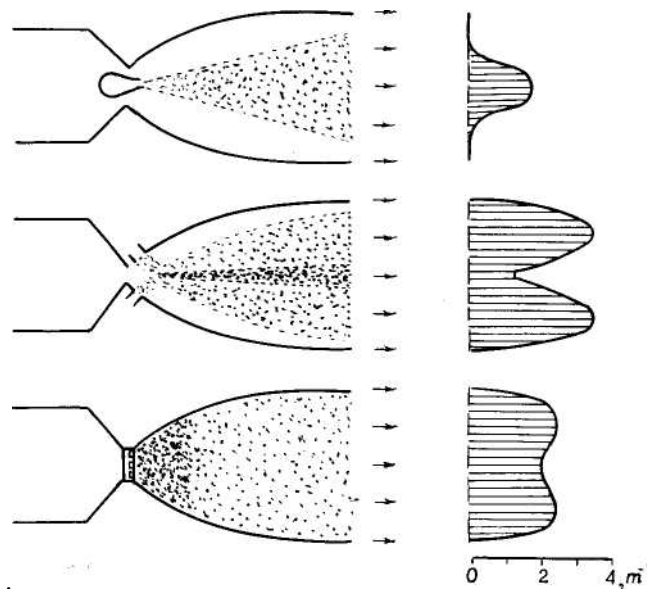


Fig. 6. Typical downstream mixing regimes and gain distribution profiles across the GDL cavity [7, 8]

All these schemes were shown to be effective. Their common basic characteristic is the double-step freezing concept, in which partial freezing of the hot nitrogen is provided prior to its mixing with cold CO_2 in order to prevent collisional deactivation effects during mixing. Thereafter, a further expansion in the GDL nozzle completes the freezing of the whole mixture. In the third of the schemes shown in Fig. 6, the first step of the N_2 expansion and partial freezing takes place between circular slotted injection tubes mounted as an array in the throat region of the main nozzle, see Fig. 7. This scheme provides rather uniform distribution of the small-signal gain coefficients across the laser cavity [8].

It is instructive to calculate the vibrational energy and population densities in the flow field of the mixing GDL nozzle and cavity. A model for the kinetics of the vibrational system [3, 4, 49–51] combined with a simplified gas-dynamic scheme of the process allows one to examine

basic features of the downstream mixing concept. We assume that (i) no losses of the nitrogen vibrational energy occur prior to the mixing area, (ii) the downstream mixing process is instant, and (iii) the flow field is hydrodynamically regular and quasi-one-dimensional.

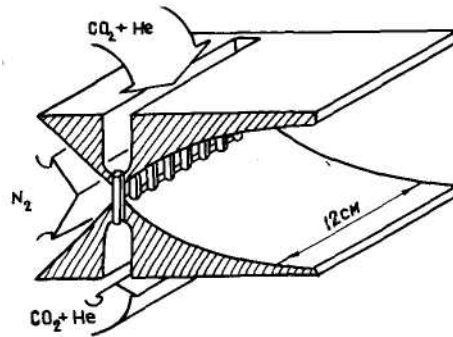


Fig. 7. Schematic drawing of $\text{CO}_2\text{-He}$ injection through a slotted tube-array [8, 48]

Then the temperature and gain profiles for a particular nozzle geometry can be obtained by numerical calculations as shown in Fig. 8.

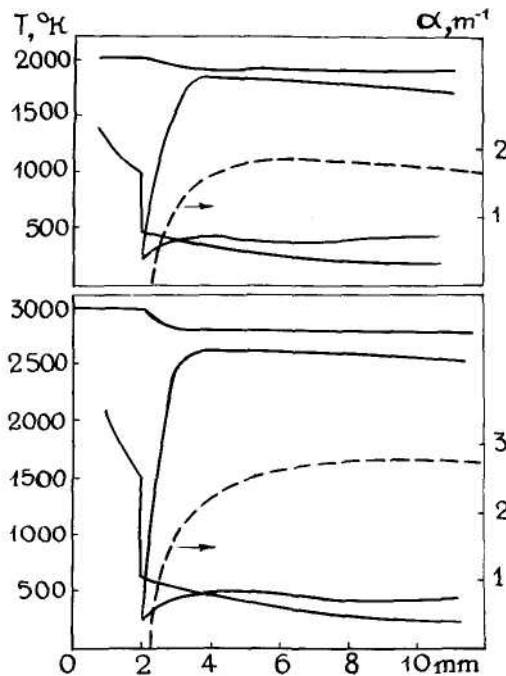


Fig. 8. Calculated temperature and gain profiles in a downstream mixing GDL: 1 = 2 mm, a mixture, $\text{CO}_2 + 9 \text{ He}$, injected at stagnation pressure 9 atm; $P_{\text{N}_2} = 10 \text{ atm}$. The resultant gas compositions are as follows: $0.033 \text{ CO}_2 + 0.67 \text{ N}_2 + 0.297 \text{ He}$ at $T_0 = 2000 \text{ K}$, and $0.055 \text{ CO}_2 + 0.452 \text{ N}_2 + 0.493 \text{ He}$ at $T_0 = 3000 \text{ K}$

The calculation results show significant temperature fall effects after the mixing with a cold gas is proceeded, highly pronounced dependences of gain coefficients both on the initial nitrogen temperature and on the injected mixture composition. However, rather weak dependences are

predicted of the specific frozen vibrational energy on the injection distance, l , within a range, $2h < J < 8h$. It should be noted that our experimental results for gain [45] correspond well to these calculations. The calculated available specific laser energies are shown in Fig. 9 as a function of plenum temperature of nitrogen. It is assumed that either (1) all vibrational levels of N_2 are effectively, used in the vibrational pumping or (2) only the first level is included in the V-V energy exchange model.

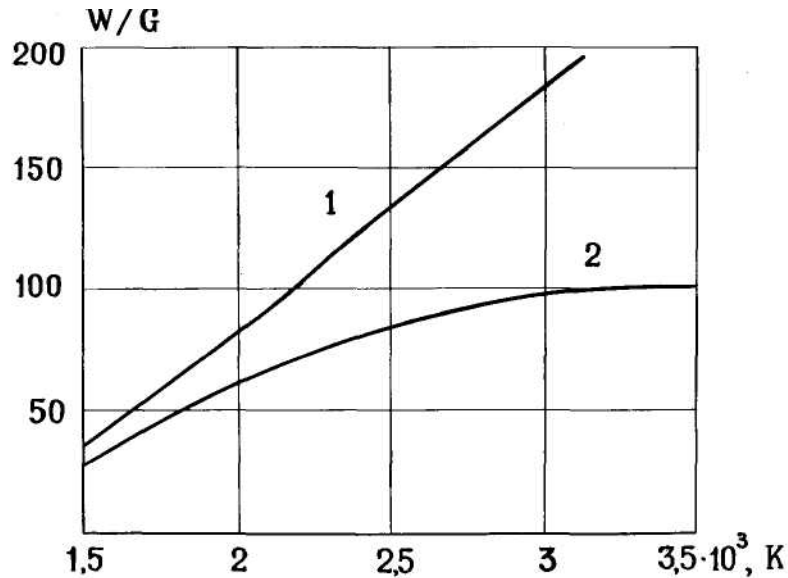


Fig. 9. Calculated available specific laser energy as a function of plenum temperature of nitrogen : (1) all vibrational levels contribute and (2) only the energy of the first vibrational level of N_2 is counted

The values obtained were multiplied by a factor of 0.8 evaluated to be maximum energy transformation efficiency within the cavity.

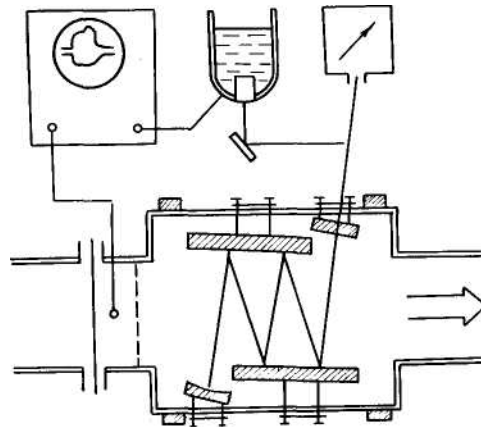


Fig. 10. Schematics of a multipass mirror system in a downstream mixing GDL [48]

Efficient conversion of the stored vibrational energy into coherent radiation requires special attention to the cavity arrangements and its optics quality. By using a multipass mirror system shown in Fig. 10, we were able to extract of about 25 % of energy available from a shock tube downstream mixing laser [48].

The experimental results are shown in Fig. 11 where the output power and the specific output energy are plotted as a function of nitrogen plenum pressure at $T_0=2000$ K.

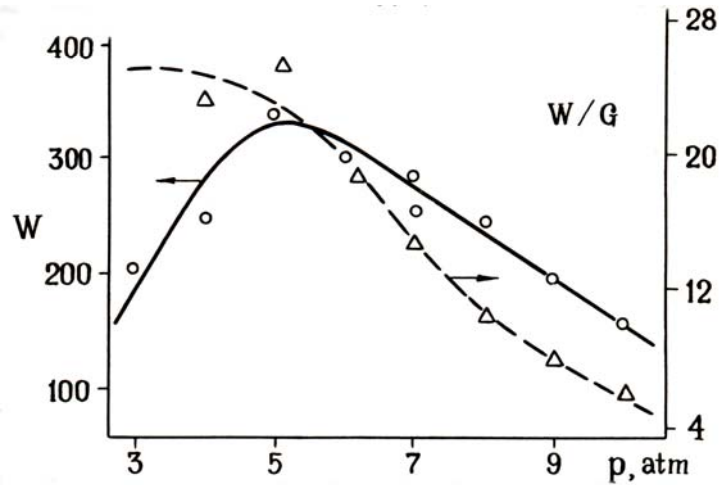


Fig. 11 . Laser output power as a function of nitrogen plenum pressure;
 $T_0 = 2000$ K; $h_* = 0.25$ mm; $\text{CO}_2:\text{He}=1:10$

It is seen that specific laser energies as high as 25J/g are extracted at evaluated maximum stored energy of about 1000J/g . This value is to be considered as one of the highest parameters attained up to date in GDLs. For comparison, basic parameters of the latest downstream mixing GDL performances are collected in Table 1. Their comparison with parameters of the premixed GDL devices also illustrate high potentialities of the downstream mixing concept.

There exist several attempts to improve efficiencies of thermally driven molecular gas lasers. Among them, the carbon monoxide GDL should be mentioned first [52–54]. Though efficiencies only of about 0.2% were attained in a CO GDL device, its capability seems not being exhausted. An interesting approach is associated with a possible use of pumping and radiant molecules with low-lying vibrational levels. In this case a laser operates at relatively low temperatures but at high quantum efficiencies. For example, a system composed of CS_2 and a suitable activating partner, $\text{CO}_2(v=1)$, $\text{O}_2(v=1)$ or $\text{CO}(v=1)$ is proposed [55] as an appropriate system with lower laser and pumping levels as compared to CO_2 or N_2O . The calculation for the CS_2 molecule shows that the inversion should occur for a number of transitions in the region of $11.4\text{--}117.0\ \mu$. The highest efficiency of 10% taking into account the relaxation losses may be attained.

We are not considering here numerous chemical laser performances. The shock tube has been exploited extensively in their developments [6]. Finally, the recombination and hybrid electric excitation principles employing fast flows of the working substance are to be considered as promising ways to develop compact and efficient flow laser devices [56, 57].

LASER-MEDIUM STUDIES

Cavity shock and rarefaction waves, shear layers and thermalized cold or hot resonance light absorbing gas samples present in a laser cavity can result in significant losses in the gain and power of fast flow lasers [2, 24, 58, 59]. To study these effects, shock tubes have proved invaluable tools for simulating of the corresponding flow conditions and thermal regimes. Figure 12 shows

schematics and experimental results obtained in studies of spatial gain distribution behind standing shock or rarefaction waves.

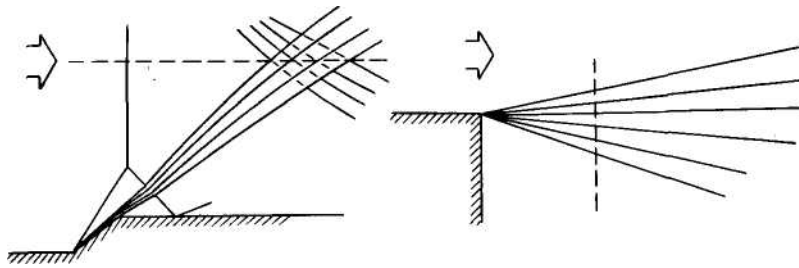


Fig. 12. Spatial gain distributions measured behind standing shock (S) and rarefaction (R) waves. Gas mixture composition $\text{CO}_2+4\text{N}_2+5\text{He}$, flow Mach number; $M = 4.7$; $p_1 = 0.01$ atm; $T_0 = 1600$ K. The dotted lines show the area of measurements

The gasdynamic disturbances were generated in a supersonic shock tube flow simulating typical conditions in a GDL cavity [61]. A conventional electric CO_2 laser (P18) was used as a probe laser in gain measurements. Its spectrum, in principle, can differ from the lasing gas spectrum, and certain corrections should be provided to treat the results of gain measurements carefully as discussed in [62]. Gain suppression or amplification effects caused by shock or rarefaction waves propagating in an inverted gas can be evaluated theoretically [61, 63]. Although a fast increase of the gas density in a shock wave can result in an increase of gain (Doppler line broadening) or in an additional freezing of a partly equilibrated lasing gas sample that passes through a rarefaction wave, shock tube experiments showed that the first of these effects is usually overlapped by molecular collisional deactivation effects, which suppresses the optical gain due to increase in gas temperature and density. In the latter case, the decrease of gain with density in a rarefaction wave is not "compensated" by the positive freezing action. Thus in both cases, the gain coefficient is continuously decreased after the initially frozen lasing gas sample passes the gasdynamic disturbance. This evidence is in a good accord with theoretical predictions of the expecting gain suppression effects.

Thermalized and thus laser light absorbing gas samples, usually present in the mirror mounting "hollows" within a laser cavity, can also lead to unfortunate effects in laser operation. Although the resonance light absorption coefficients can be properly evaluated theoretically as a function of gas temperature and density [64–69], certain difficulties exist in their precise calculations based on analyses of all the elementary absorption mechanisms that contribute to the light absorption at moderate gas densities and at temperatures ranging between 500 K and 2000 K that are typical for a gasdynamic laser. Shock tube measurements of the resonance (10.6μ) laser beam absorption coefficients in shocked CO_2 and in a $\text{CO}_2\text{-N}_2$ mixture permits the comparison of the experimental data with their theoretical predictions in a wide temperature range [70, 71]. The results are shown in Fig. 13 where the absorption coefficient has been measured with use of a $J=18$ CO_2 laser line beam absorbed in a shocked gas sample behind the incident shock wave propagating in a 5×5 cm² shock tube operated for IR absorption measurements.

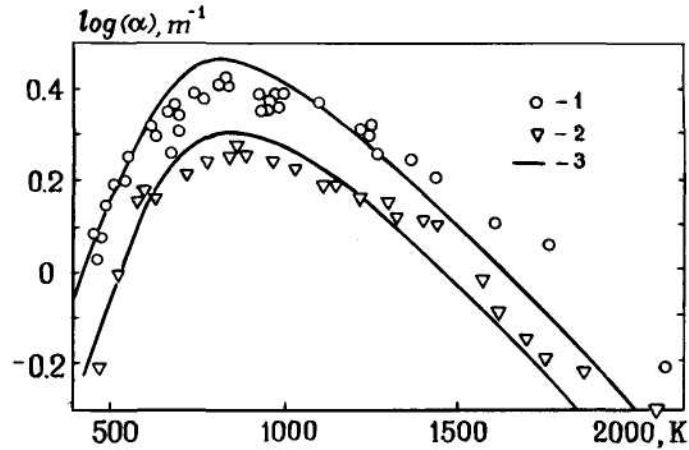


Fig. 13. Resonance absorption coefficient as a function of temperature in pure CO₂ (1) and in CO₂-N₂ mixture (2). Solid lines show the theoretical temperature dependence of the total absorption coefficient at 10.6 μ . Shocked gas pressure, $p_S = 3$ atm

It is seen that fairly good agreement can be reached between the calculated (the collisional broadening cross-section, $\sigma_c \sim T^{-1/2}$) and measured values of the absorption coefficient in a shock heated CO₂ and in CO₂-N₂ mixture. Note in addition that the resonance laser light absorption coefficients were also measured in shocked CH₄ (3.39 μ) [72], SF₆(10.6 μ) [73], and C₃H₈(10.6 μ). Very high values of the absorption coefficient in propane are measured in our recent experiments.

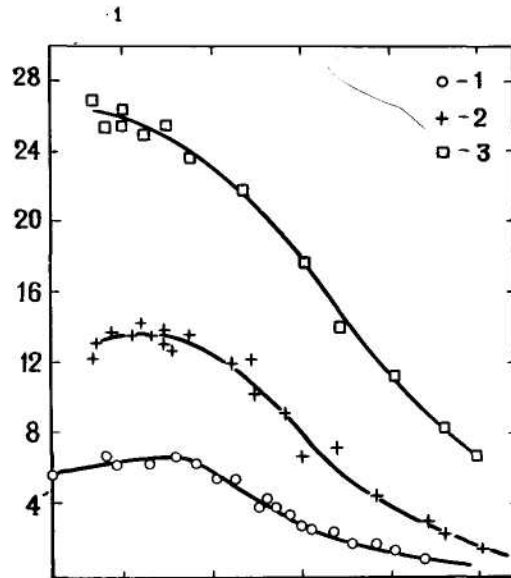


Fig. 14. Absorption coefficient in C₃H₈+9Ar as a function of temperature. Shocked gas pressure: (1) -1 atm, (2) - 2-3 atm, (3) - 3-5 atm

Figure 14 shows the results of these measurements. More than 10 near-resonant transitions were found to contribute to the IR light absorption at high and ambient temperatures.

CONCLUDING REMARKS

It should be stressed in conclusion that the above considerations and examples clearly demonstrate a high capability of the shock tube in the modeling of high temperature fluid mechanic and optical phenomena associated with complicated processes of molecular and radiative energy transfer. On the other hand, when basic properties of the non-equilibrium gas flow field in the gasdynamic lasers are better understood, an opportunity can be provided by an experimental apparatus based on the use of radiation dynamics and optical properties of lasing gas flows for the measurements and critical evaluation of elementary molecular kinetic data, such as rate coefficients of vibrational energy exchanges in composite molecular system.

ACKNOWLEDGEMENTS

The author wishes to thank Yu.A.Yacobi, N.A.Fomin, V.N.Croshko, G. A. Zavarsine and O.V.Achasov for their assistance and useful discussions.

REFERENCES

1. D. A. Russel, W. H. Christiansen and A. Hertzberg, Shock Tube Lasers, Proc. 8th Intern. Shock Tube Symp., Chapman and Hall, London, 1971.
2. W. H. Christiansen, D. A. Russel and A. Hertzberg, Flow Lasers Ann. Rev. Fluid Mech. **7**, 115 (1975).
3. J. D. Anderson, Gasdynamic Lasers: an Introduction, Academic Press, 1976.
4. V. K. Konyukhov, Quant. Electronica **4**, 5 (1977).
5. B. R. Bronfin, Continuous Flow Combustion Lasers, Fifteenth Symp. (Intern.) on Combustion, p.935, The Combustion Institute, Pittsburgh, 1974.
6. R. W. F. Gross and J. F. Bott (Eds.), Handbook of Chemical Lasers, A Wiley-Interscience Publication, 1976.
7. V. N. Croshko, R. I. Soloukhin and N. A. Fomin, Fiz. Goreniya i Vzryva **10**, 473 (1974).
8. V. N. Croshko, R. I. Soloukhin and N. A. Fomin, Acta Astronautica **2**, 929 (1975).
9. A. P. Doronov et.al., Soviet JETP (Pis'ma v Red.) **11**, 516 (1970).
10. A. I. Demin et.al., Quant. Electronica **3(9)**, 72 (1972).
11. A. S. Biryukov et.al., High Temperature-High Pressures **5**, 389 (1973).
12. D. M. Kuehn and D. J. Monson, Appl. Phys. Letters **16**, 48 (1970).
13. W. H. Christiansen and G. A. Tsongas, Phys. Fluids **14**, 2611 (1971).
14. S. A. Losev et.al., Fiz. Goreniya i Vzryva **4**, 463 (1973).
15. V. R. Buonadonna and W. H. Christiansen, Proc. 9th Intern. Shock Tube Symp., p. 173, Stanford Univ. Press, 1973.
16. E. L. Klosteiman and A. L. Hoffman, Proc. 9th Intern. Shock Tube Symp., p. 156, Stanford Univ. Press, 1973.
17. D. A. Russel and V. R. Buonadonna, Proc. 9th Intern. Shock Tube Symp., p.238, Stanford Univ. Press, 1973.
18. A. K. Oppenheim, P. A. Urtiew and A. J. Lademan, Archiwum Budowy Maszyn (Warszawa) **11** 441 (1964).
19. V. N. Croshko, R. I. Soloukhin and N. A. Fomin, Fiz. Goreniya i Vzryva **3**, 352 (1973).
20. E. T. Gerry, IEEE Spectrum **7**, 51 (1970).
21. D. M. Kuehn, Appl. Phys. Letters **21**, 112 (1972).
22. R. A. Greenberg et.al., AIAA J. **10**, 1494 (1972).
23. J. D. Anderson and E. L. Harris, Laser Focus **5**, 32 (1972).

24. D. A. Russell, AIAA Paper № 74-223 (1974).
25. D. A. Russell, S. E. Neice and P. H. Rose, AIAA J. **13**, 593 (1975).
26. J. Tulip, H. Seguin, Appl. Phys. Letters **19**, 263 (1971).
27. G. Lee, F. E. Gowen and J. R. Hagen, AIAA J. **10**, 65 (1972).
28. N. A. Generalov et.al., Zh. Prikl. Mekh. Tekhn. Phys. **5**, 24 (1971).
29. A. L. Hoffman and G. C. Vlases, IEEE J. **QE-8**, 2, 46 (1972).
30. G. C. Vlases, Laser Interaction and Related Plasma Phenomena, Eds. H. J. Schwarz and H. Hora, p. 25, Plenum Press, 1972.
31. S. S. R. Murty, AIAA Paper №. 74-226 (1974).
32. S. A. Munjee, Phys. Fluids **15**, 506 (1972).
33. S. A. Losev and V. N. Makarov, Quant. Electronica **7**, 1633 (1974).
34. G. Lee, Phys. Fluids **17**, 644 (1974).
35. A. P. Napartovich and V. F. Sharkov, Teplofizika Vysokikh Temperatur **3**, 659 (1974).
36. K. Kasuya et.al., Proc. 10th Intern. Shock Tube Symp., p. 107, Kyoto University, 1975.
37. I. R. Hurler and A. Hertzberg, Phys. Fluids **8**, 160 (1965).
38. V. K. Konyukhov and A. M. Prokhorov, Soviet JETP (Pis'ma v Red.) **3**, 436 (1966).
39. M. S. Dzhidzhoev et.al., Soviet JETP (Pis'ma v Red.) **13**, 73 (1971).
40. S. Yatsivet.al., Appl. Phys. Letters **19**, 65 (1971).
41. J. Tulip and H. Seguin, Appl. Phys. Letters **19**, 263 (1971).
42. N. N. Kbudriavtsev, S. S. Novikov and I. B. Svetlichnyi, Zh. Prikl. Mekh. Tekhn. Fiz. **5**, 9 (1974).
43. G. I. Kozlov et.al., Zh. Tekhn. Fiz. **68**, 1647 (1975).
44. V. N. Croshko, R. I. Soloukhin and P. Wolanski, Optics Commun. **6**, 275 (1972).
45. V. N. Croshko, R. I. Soloukhin and P. Wolanski, Proc. 9th Intern. Shock Tube Symp., p. 167, Stanford Univ. Press, 1973.
46. J. Milewski et.al., Bull. Acad. Pol. Sci., Ser. Sci. Techn. **20**, 73 (1972).
47. J.-P. E. Taran, M. Charpenel and R. Borghi, AIAA Paper. No 73-622 (1973).
48. A. V. Krauklis et.al., Fiz. Goreniya i Vzryva **5**, 792 (1976).
49. R. L. Taylor and S. Bitterman, Rev. Mod. Phys. **41**, 26 (1969).
50. A. S. Biryukov, Proc. P. N. Lebedev Institute of Physics, USSR Acad. Sci. **83**, 13 (1975).
51. J. D. Anderson, AIAA J. **12**, 1699 (1974).
52. R. L. McKenzie, Phys. Fluids **15**, 2163 (1972); also: Appl. Phys. Letters **17**, 462 (1970).
53. W. S. Watt, Appl. Phys. Letters **18**, 487 (1971).
54. R. E. Center and G. E. Caledonia, Appl. Optics **10**, 1795 (1971).
55. A. Yu. Volkov et.al., Quant. Electronica **3**, 1833 (1976).
56. B. Forestier, B. Fontaine and J. Valenci, Proc. 10th Intern. Shock Tube Symp., p. 99, Kyoto University, 1975.
57. B. Forestier et B. Fontaine, Institute de Mechanique des Fluides de Marseille, Janvier 1976.
58. G. A. Simons, AIAA J. **9**, 1417 (1971).
59. O. Biblarz and A. E. Fuhs, AIAA J. **12**, 1083 (1974).
60. A. L. Hoffman and T. G. Jones, AIAA Paper No. 72-217 (1972).
61. R. I. Soloukhin and N. A. Fomin, Doklady AN SSSR **228**, 596 (1976).
62. R. I. Soloukhin and Yu. A. Yacobi, Zh. Prikl. Mekh. Tekhn. Fiz. **3**, 4 (1974).
63. G. I. Kozlov and E. L. Stupitskii, Zh. Tekhn. Fiz. **45**, 359 (1975).
64. E. T. Gerry and D. A. Leonard, Appl. Phys. Letters **8**, 111 (1966).
65. W. H. Christiansen, G. L. Mullaney and A. Hertzberg, Appl. Phys. Letters **18**, 385 (1971).

66. R. Ely and T. K. McGubbin, *J. Appl. Optics* **9**, 1230 (1970).
67. R. L. Leonard, *J. Appl. Optics* **13**, 1920 (1974).
68. S. A. Munjee and W. A. Christiansen, *J. Appl. Optics* **12**, 993 (1973).
69. J. L. Miller and E. V. George, *Appl. Phys. Letters* **27** 665 (1975).
70. A. R. Strilchuk and A. A. Offenberger, *J. Appl. Optics* **13**, 2643 (1974).
71. R. I. Soloukhin and N. A. Fomin, *Zh. Prikl. Mekh. Tekhn. Fiz.* **1**, 42 (1977).
72. R. J. Emrich and R. I. Soloukhin, *Acta Astronautica* **17** 639 (1972).
73. A. V. Novak and J. L. Lyman, *J. Q. S. R. T.* **15** 945 (1975).
74. G. V. Abrosimov et.al., *Teplofizika Vysokikh Temperatur* **13**, 865 (1975).
75. P. E. Cassady, J. Newton and P. Rose, *AIAA Paper No.* 76-343 (1976).
76. W. Schall, P. Hoffman and H. Hugel, *J. Appl. Phys.* **48**, 688 (1977).
77. R. A. Meinzer, *AIAA Paper No.* 71-25 (1971).
78. V. G. Testov et.al., *Soviet JETP* **71**, 88 (1976).